

Towards Microfluidic Separation Processes using Switchable Hydrophilicity Solvents

Margaux Zollo*, Jean-Baptiste Salmon, Yaocihuatl Medina-Gonzalez

Laboratoire du Futur (CNRS, Solvay, Université de Bordeaux, UMR 5258), 178 avenue du Dr. Albert Schweitzer- 33600 Pessac, France.
margaux.zollo-ext@solvay.com

CO₂ - Switchable Hydrophilicity solvents (SHS) are liquid solvents that are highly hydrophobic at room conditions and become hydrophilic when exposed to CO₂; this phenomenon is, in most cases, reversible. This class of solvents has gained popularity because they offer opportunities in many processes such as liquid-liquid separations. In this work, a CO₂ - SHS, 2-2-Dibutylaminoethanol (DBAE), was chosen to study the switching phenomenon using polydimethylsiloxane (PDMS) microfluidic devices made by soft lithography. The compatibility of this solvent with PDMS was tested by observations at the scale of a centimetric piece of PDMS, and at the scale of a microfluidic channel (approx. 50 μm in height). No visible swelling of the polymer matrix was observed on a macroscopic scale, while we demonstrated DBAE pervaporation, PDMS oligomer extraction, and accumulation of a fluorescent compound at the microfluidic channel scale.

1. Introduction

The development of environmentally friendly and sustainable chemical processes is often limited by the choice of the optimal solvent, which is often a non-trivial task. Indeed, most common chemical processes are often multi-step processes involving reactions, extractions, and separations. Each reactant, catalyst and chemical involved has a different solubility, which means that a different solvent is needed to solvate each component of the process. The optimal choice of a solvent is limited because most solvents have fixed physical properties (Jessop, 2015). In this context, solvent engineering aims at controlling the solubility and transport properties of a solvent medium, in order to optimize the chemical or physical processes performed.

Among the strategies of solvent engineering, reversible CO₂ - switchable hydrophilicity solvents (CO₂ - SHSs) represent a promising route to reversibly change the properties of a solvent. CO₂ - SHSs are usually liquid solvents that are normally very hydrophobic and therefore form a biphasic mixture when mixed with water. However, when exposed to CO₂, they become hydrophilic and completely miscible with water. By removing the CO₂ from the system, for example by heating or N₂ bubbling, the solvent returns to its hydrophobic form. This new generation of solvents has gained popularity for many processes: highly selective sequential extractions, catalytic reactions, and synthesis of advanced materials (Boyd, et al., 2012). In particular, CO₂ - SHSs offer interesting opportunities for multistep separation processes for which the use of different solvents makes the process environmentally unfriendly and energy intensive (Samori, et al., 2010).

Microfluidics is a widely used toolbox to manipulate liquids at the nanoliter scale in networks of microfabricated channels with typical transverse dimensions ranging from 10 to 100 μm. The advantages of the microfluidic scale are not only related to the small volumes of liquids handled, but also to the possibility of tightly controlling the transport phenomena (mass/energy/charges) due to the small channel dimensions. In this context, the coupling of microfluidic tools and SHS constitutes a new opportunity to develop efficient liquid-liquid separation processes. Studies involving SHSs in microfluidic applications have already been reported by some groups. For example, Han, et al. (2021) exploited the permeability of Teflon microtubing to gases to study the extraction and recovery rates of a given SHS and to compare it to macroscopic batch conditions. Lestari, et al. (2017) also studied oil extraction and the solvent recycling capacity of SHSs by putting a drop in a tubing and submitting it to an oscillatory motion in a CO₂ or N₂ atmosphere.

However, these studies were mostly demonstrations at a millifluidic scale inside millimetric tubes, but we are not aware of studies involving SHS in standard networks of microfluidic channels, with typical channel dimensions ranging from 10 to 100 μm . Among the materials constituting microfluidic chips, polydimethylsiloxane (PDMS) is the most common, primarily due to the ease of microfluidic chip fabrication using soft lithography techniques. PDMS is also a material of choice in microfluidic applications because it is permeable to gases, including CO_2 and N_2 . This property offers unique opportunity in the context of SHSs to tune the hydrophobicity of a solvent flowing in a microfluidic PDMS chip by exploiting the permeability of PDMS to CO_2 and N_2 . Nevertheless, PDMS is also a material known for its poor compatibility with many organic solvents, and we are not aware of any work that has studied its possible compatibility with SHSs. The goal of this work is to elucidate this point using observations at both the macroscopic scale (a centimetric block of PMDS) and at the microchannel scale, on a given SHS, 2,2-Dibutylaminoethanol (DBAE).

2. Materials and methods

2.1 Choice of the system: 2,2-Dibutylaminoethanol (DBAE)

Typically, switchable solvents are organic super-bases such as 1,8-Diazabicyclo(5.4.0)undec-7-ene (DBU). DBU is not an SHS per se and requires specific additives or complex formulations to acquire the switching capability, as the introduction of ions (Zidong, et al., 2020) or the addition of amino acids (Carrera, et al., 2015) or alcohols (Samori, et al., 2010). Also, for these chemicals, the reversible switch phenomenon cannot be observed under ambient conditions and requires higher temperatures. In this work, the switching of some SHSs already known in the literature (Vanderveen, et al., 2014), DBAE, DBU, triethylamine, DBU + alcohol and/or acetate, 1,5-Diazabicyclo(4.3.0)non-5-ène + alcohol and/or acetate, were tested through CO_2 and N_2 bubbling under ambient conditions (all the chemicals were purchased from Sigma Aldrich). For each solvent, vials containing different volumes of water and solvent were prepared and bubbled initially with CO_2 to observe the hydrophilicity switch. CO_2 flow was controlled using Bronkhorst® mini CORI-FLOW™ digital mass flow meter with an inlet pressure of 3 bar and van opening between 10-20%. Then, once the phase change was obtained, the reversibility of the reaction was tested through N_2 bubbling (1 bar).

Figure 1 shows the system DBAE-Water (50% volume fraction, $V_{\text{DBAE}}/V_{\text{TOT}}$) before and after bubbling of CO_2 . Before bubbling with CO_2 , both solvents are non-miscible as shown by the meniscus separating the two liquids (DBAE is less dense than water). After bubbling CO_2 (duration 180 min), both solvents mix and do not separate again. As shown in Figure 1, bubbling N_2 (duration 270 min), makes it possible to separate again the two solvents. Among the other systems tested, DBAE-Water was the only one able to switch its hydrophilicity at ambient temperature and pressure.

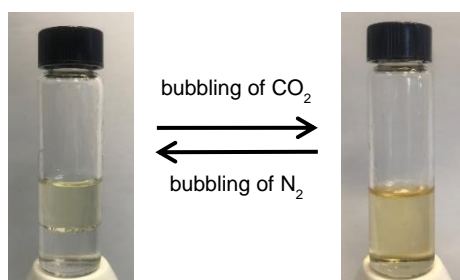


Figure 1: Image of the switch obtained at ambient condition for the system DBAE-Water (50% $V_{\text{DBAE}}/V_{\text{TOT}}$). The volume of liquids in the experiment is around 4 mL, the time required is 180 min for the CO_2 bubbling and 270 min for N_2 bubbling.

The time required to obtain the monophasic mixture through CO_2 bubbling and the time required for the same system to come back to its biphasic condition (through N_2 bubbling) increase with increasing DBAE/ H_2O volume ratio $V_{\text{DBAE}}/V_{\text{TOT}}$. Typically, from 20 min to 180 min for the CO_2 bubbling for ratios ranging from 0.2 to 0.5. Moreover, the N_2 bubbling time was always larger than the CO_2 bubbling time (typically from 50 min to 270 min). This suggests that the kinetics of the forward reaction is faster than that of the backward reaction. It is also worth noting that this type of testing has been carried out on total volumes ranging between 1 and 8 mL that are much larger than those that will be used in microfluidic experiments discussed below ($< 1 \mu\text{L}$). Thus, the kinetics of these processes can be expected to be greatly reduced for smaller volumes.

2.2 Fabrication of microfluidic chips

The microfluidic devices were fabricated using standard soft lithography techniques starting from a negative photoresist mold (SU-8 3050, MicroChem) made by classic lithography. In brief, the SU-8 master with relief microchannels was placed in a petri dish and molded with a mixture obtained by mixing PDMS prepolymer (Sylgard-184) and its curing agent (10:1 mass ratio) previously de-gassed under vacuum at room temperature. Polymerization of the PDMS mixture was then activated at 65°C in an oven (typically for 2 h). After peeling the PDMS cross-linked layer from the SU-8 mold and punching it to make openings, a plasma treatment was used to covalently seal a glass slide onto the PDMS block, thus ensuring a perfect seal of the channel array. Once the microfluidic chip is obtained, flows of chemicals in the channels are imposed using pressure controllers (MFCS, Fluigent) that control the inlet pressure. The height of the microfluidic channels were measured from the SU8 mold using an optical profilometer with an interferometric acquisition setting (Sensofar Non-contact 3D Optical Profiler, objective lens: 10X Nikon DI).

3. Results and discussion

3.1 Macroscopic observations

*Preliminary macroscopic observations were carried out because no information on the compatibility of the PDMS material with DBAE was found in the previous literature (Lee, et al., 2003). **Errore. L'origine riferimento non è stata trovata.** describes the macroscopic experiment performed: a PDMS block of known dimensions is placed in a vial containing DBAE (typical volume around 15 ml) at room temperature and pressure. After around 2 months, the cube was removed from the vial, and its dimensions were measured again. The result is a slight color change, but no measurable swelling. This means that DBAE did not significantly swell the PDMS matrix, and thus suggests that PDMS is a priori compatible with this solvent.*

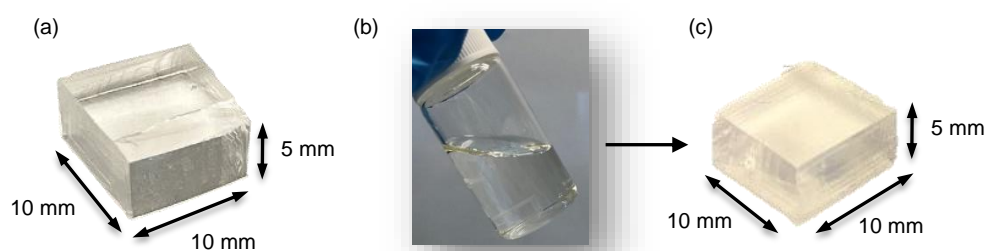


Figure 2: Representation of the macroscopic experiment: a block of PDMS of known dimensions (a) was immersed in a vial (15 ml) containing DBAE (b). After 2 months at ambient conditions, the block was taken out from the liquid and was not significantly swelled (c).

3.2 Observations at the microfluidic scale

To further investigate the compatibility between DBAE and PDMS, micro-scale observations were performed. In a first step, a single dead-end microfluidic channel, as schematically shown in Figure 2 (width 400 μm , height 50 μm , length 3 cm) was filled with DBAE. Indeed, the gas permeability of PDMS allows to easily fill a channel without outlet with a liquid by applying a moderate pressure at the channel inlet (100-400 mbar). Once the channel was completely filled, the inlet pressure was released, and the evolution of the microchannel was observed for about 20 hours under a microscope equipped with epifluorescence.

Pervaporation

The first observation made was the significant drop in the level of liquid DBAE in the inlet tube, corresponding to a volume loss of about 65 μL in about 20 hours. In addition, we observed this same phenomenon by preventing evaporation of DBAE into the air at the tubing inlet with a fluorinated oil plug (FC40, 3M). This observation suggests that DBAE molecules continuously solubilize into the PDMS matrix, diffuse, and then evaporate in ambient air, which is called the pervaporation phenomenon. The DBAE mass flux imposed by its pervaporation through PDMS leads to a continuous flow inside the channel. This phenomenon was widely described for aqueous solution in PDMS chips, as water is also slightly soluble in PDMS (Bacchin, et al., 2022). The rough measurement of the DBAE volume loss in the tube leads to an estimate of the pervaporation rate of about 10 nL/min in the configuration of Figure 2.

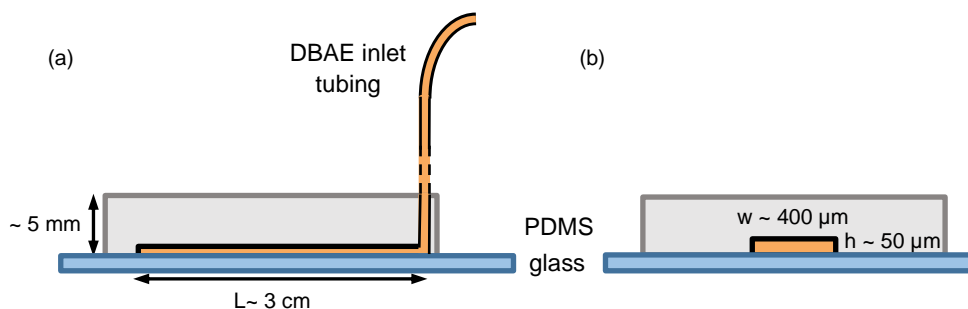


Figure 2: Side (a) and front (b) section of the designed microfluidic channel.

In order to better characterize this phenomenon, the following experiment was performed. The microchannel was first filled as explained above. Once the channel is fully filled, the inlet tube is disconnected and a liquid plug of fluorinated oil is placed at the inlet of the chip to prevent evaporation of DBAE into air from the chip inlet. Figure 3a shows several snapshots of the microfluidic channel, over around 7 h of observation. These images allow to reveal without ambiguity the emptying of the channel over time. Because the FC40 plug prevent DBAE evaporation from the inlet, these observations again suggest DBAE pervaporation corresponding to the solubilization of DBAE within the PDMS, its diffusion through the solid matrix, and its evaporation into ambient air.

Figure 3b shows the local meniscus velocity against its position along the canal, obtained by tracking the meniscus over time. The meniscus velocity v varies linearly between 0 and $5.4 \mu\text{m/s}$ at the inlet, corresponding to flow rates $(hw)v = 6.5 \text{ nL/min}$ compatible with the measurements from the meniscus level in the tube.

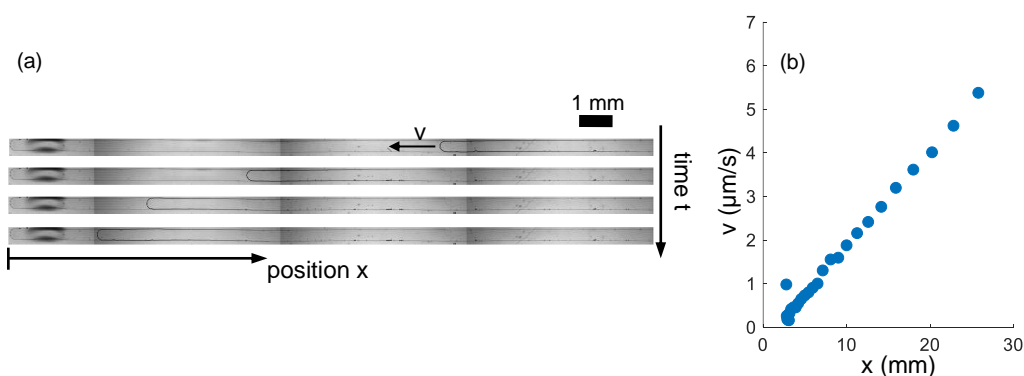


Figure 3: Emptying of the microfluidic channel initially full of DBAE over time: meniscus moving along the x position (a), plot of the speed ($v=-dx/dt$) over x (b). The frames in (a) are composite images the microfluidic channel, obtained by moving the microscope stage. The channel has a deformation at its end (position $x=0$).

The linear decrease of the meniscus velocity shows that the pervaporation flux increases linearly with the length of the channel filled with DBAE, and thus suggests a 1D description of pervaporation in the geometrical configuration of Figure 2. Similar results were also found both experimentally and theoretically for pervaporation of water in linear PDMS microfluidic channels (Bacchin, et al., 2022).

Dollet, et al. (2019), provided analytical formulae predicting the pervaporation rate from a rectangular channel, in a configuration close to Figure 2, assuming for simplicity a constant diffusivity D of the solvent in the PDMS matrix, and Henry's law for its solubility up to C (kg/m^3). With these assumptions and the theoretical predictions from Dollet, et al. (2019), it's possible to predict the value of the product $C \cdot D$ knowing the pervaporation flow rate and the transverse dimensions of the channel. The measurements of Figure 3a lead to the following estimate for the product $C \cdot D = 9.5 \times 10^{-10} \text{ kg}/(\text{m s})$. This value compares to $C \cdot D = 7.7 \times 10^{-10} \text{ kg}/(\text{m s})$ in the case of pure water. Independent measurements of the DBAE solubility in PDMS could a priori allow us to deduce the diffusion coefficient of DBAE in PDMS from these measurements.

Fluorescence accumulation and phase separation

At the microscopic scale, Figure 4 shows typical images of the tip of the channel at different times. Initially, the channel is homogeneously filled by DBAE (Figure 4a). Then, we observed the formation of small droplets after

typically 6 hours (Figure 4b), their movement towards the end of the channel, and finally their coalescence leading to phase separation (Figure 4c). It is also important to mention that one of the phases seems to wet the PDMS matrix significantly better than the other phase. Raman micro-spectroscopy performed in the channel (data not show) also revealed that this last phase displays a Raman signature close to that of the PDMS matrix. Fluorescence imaging (excitation 480 nm, emission 520 nm) simultaneously reveals a continuous increase of the fluorescence intensity at the channel tip. Thus suggesting the continuous accumulation of a fluorescent compound, see Figure 4d. These images also reveal that the phase that preferentially wets the PDMS does not contain these fluorescent compounds. All these observations, combined with the continuous DBAE pervaporation revealed previously, suggests different phenomena as explained below.

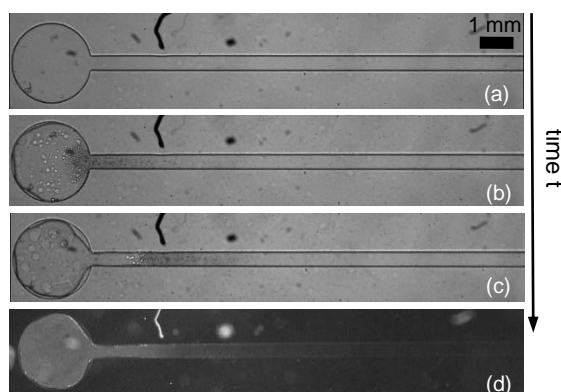


Figure 4: Evolution of the tip of the channel over 20 hours of observation with (a-c) visible light and (d) fluorescence microscopy ($\lambda_{ex} \approx 488 \text{ nm}$, $\lambda_{em} \approx 530 \text{ nm}$). Times are 0, 6, 20, and 20 h for (a), (b), (c), and (d).

Oligomers extraction linked to pervaporation

Figure 5(a-c) schematically illustrates the hypothesis put forward to describe the phase separation observed at the channel tip. DBAE in the channel continuously extracts un-cross-linked PDMS oligomers from the bulk of the PDMS matrix, as previously reported for many other organic solvents (Lee, et al., 2003) (Figure 5a). The flow induced by pervaporation in the channel then transports these extracted oligomers up to the channel tip, where they continuously accumulate (Figure 5b).

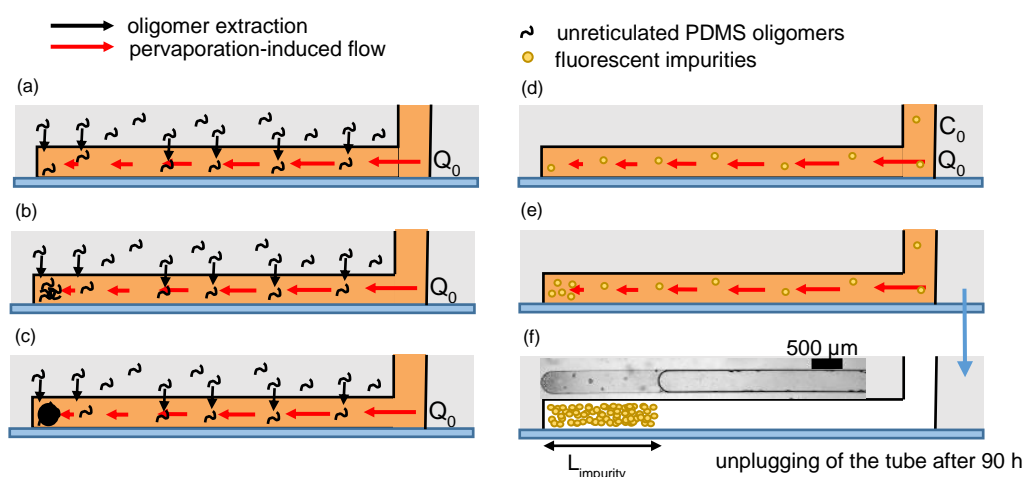


Figure 5: Schematic scenario of the continuous oligomer extraction and their accumulation up to phase separation (a-c), and the pervaporation-induced accumulation of a fluorescent impurity contained in DBAE (d-f).

Above a critical concentration, these oligomers are not soluble anymore and form a distinct phase (appartition and coalescence of droplets, Figure 5c) that preferentially wet the PMDS walls of the chip because of its chemical affinity. This scenario was further confirmed with experiments in which the chip was firstly pre-washed

with DBAE, in order to extract PDMS oligomers, as in (Lee, et al., 2003). For these experiments, we do not observe anymore the phase separation shown in Figure 4, thus confirming the scenario shown in Figure 5.

Fluorescent compound accumulation

In the same way, see Figure 5(d-e), the pervaporation-induced flow is capable of continuously accumulate any impurities up to the channel tip, in the case this impurity is not soluble in PDMS. The observation of the continuous increase of the fluorescence intensity at the end of the channel could be due to this same phenomenon, in the case of a fluorescent impurity contained in the solvent DBAE. In addition, the following experiment was performed. After 90 h of continuous accumulation, the inlet DBAE tube was unplugged from the chip. After complete pervaporation of DBAE, Figure 5f shows that a significant volume of the fluorescent compound remains trapped at the tip, confirming that this impurity is not soluble in the PDMS matrix. The measurement of its volume and the knowledge of the overall pervaporation-induced flow rate (see above), leads to a rough estimate of the concentration of this impurity in DBAE, below 0.5% in volume fraction.

4. Conclusion

In conclusion, we have investigated the compatibility of a hydrophilic switchable solvent 2,2-Dibutylamino ethanol, DBAE, with the most commonly used material for microfluidic chips, polydimethylsiloxane. Initial macroscopic observations suggested an apparent compatibility between the two compounds. Then, observations at the scale of a dead-end microchannel revealed DBAE pervaporation, extraction of un-crossed linked PDMS oligomers, and the presence of a fluorescent compound in DBAE. DBAE pervaporation through the PDMS matrix induces a flow towards the tip of the microfluidic channel leading to a phase separation and the continuous accumulation of the fluorescent compound. DBAE pervaporation rates in our configuration are small, around 5 nL/min, and it is probable that they can be safely neglected in other microfluidic configuration for which residence times in the channels are small. The same conclusion holds for the extraction of PDMS oligomers and the presence of the impurity revealed in the present work. In a near future, we expect to exploit the permeability of PDMS to CO₂ and N₂ to design and optimize a microfluidic liquid-liquid separation experiment using DBAE in a PDMS chip.

References

- Bacchin, P., Leng, J. & Salmon, J.-B., 2022, Microfluidic Evaporation, Pervaporation, and Osmosis: From Passive Pumping to Solute Concentration, *Chemical Reviews*, Vol 122, 6938–6985.
- Boyd, A. R. et al., 2012, Switchable hydrophilicity solvents for lipid extraction from microalgae for biofuel production, *Bioresource Technology*, Vol 118, 628-632.
- Carrera, G. V. S. M. et al., 2015, Reversible systems based on CO₂, amino-acids and organic superbases. *RSC Advances*, Vol 5, 35564-35571.
- Dollet, B. et al., 2019, Drying of channels by evaporation through a permeable medium, *Journal of The Royal Society Interface*, Vol 16.
- Han, S., Ibrahim, M. Y. S. & Abolhasani, M., 2021, Intensified recovery of switchable hydrophilicity solvents in flow, *Chemical Communications*, Vol 57, 11310-11313.
- Jessop, P., 2015, Switchable Solvents as Media for Synthesis and Separations, *Aldrichimica Acta*, Vol 48, 18-21.
- Lee, J. N., Park, C. & Whitesides, G. M., 2003, Solvent Compatibility of Poly(dimethylsiloxane)-Based Microfluidic Devices, *Analytical Chemistry*, Vol 75, 6544-6554.
- Lestari, G., Alizadehgiashi, M., Abolhasani, M. & Kumacheva, E., 2017, Study of Extraction and Recycling of Switchable Hydrophilicity Solvents in an Oscillatory Microfluidic Platform, *ACS Sustainable Chemistry & Engineering*, Vol 5, 4304-4310.
- Samori, C. et al., 2010, Extraction of hydrocarbons from microalga *Botryococcus braunii* with switchable solvents, *Bioresource Technology*, Vol 101, 3274-3279.
- Vanderveen, J. R., Durelle, J. & Jessop, P. G., 2014, Design and evaluation of switchable-hydrophilicity solvents, *Green Chemistry*, Vol 16, 1187-1197.
- Zidong, Z. et al., 2020, Preparation and Application of CO₂ -Triggered Switchable Solvents in Separation of Toluene/ n-Heptane, *Langmuir*, Vol 36, 510-519.